Electrochemical Impedance Spectroscopy-Based Electric Circuit Modeling of Lithium-Sulfur Batteries During a Discharging State

Stroe, Daniel-Ioan; Knap, Vaclav; Swierczynski, Maciej Jozef; Schaltz, Erik

Published in:
I E E E Transactions on Industry Applications

DOI (link to publication from Publisher):
10.1109/TIA.2018.2864160

Publication date:
2019

Document Version
Accepted author manuscript, peer reviewed version

Electrochemical Impedance Spectroscopy-based Electric Circuit Modeling of Lithium-Sulfur Batteries during Discharging State

Daniel-Ioan Stroe, Vaclav Knap, Maciej Swierczynski, Erik Schaltz
Department of Energy Technology
Aalborg University
Aalborg, Denmark
dis@et.aau.dk

***Abstract*—Lithium-ion batteries are characterized by having very good performance in terms of efficiency, lifetime, and self-discharge, which allowed them to become the major player in the electric vehicle applications. However, they were not able to totally overcome the EV range anxiety. Thus, research is carried out nowadays to develop batteries with even higher gravimetric energy density, which should allow a substantial range increase. One of the technologies, which should be able to meet the range requirements is the Lithium-Sulfur (Li-S) battery. Thanks to the extensive research and development efforts, these cells are close to enter the market, being evaluate in various projects. In this paper, we have proposed an electrical circuit model for a Li-S pouch cell, which was parameterized based on extensive electrochemical impedance spectroscopy measurements. The developed model was verified using static and pulse discharge profiles, showing a good accuracy in predicting the voltage of the tested Li-S battery cell.**

Keywords—Lithium-Sulfur battery, modeling, electric circuit, electrochemical impedance spectroscopy, discharging

I. INTRODUCTION

In order to meet the demanding requirements of electric vehicles (EVs) in terms of energy density and safety, battery research has followed different directions in the past decade. The Lithium-ion battery has been continuously improved since the commercialization of the first Li-ion battery in the 90s [1]. Thus, Li-ion batteries based on the NMC and NCA chemistries are nowadays the technology to choose in EV applications, mainly because of their high gravimetric energy density (i.e., 170 Wh/kg for NMC and 150 Wh/kg for NCA) and reasonable lifetime (i.e., 3000 full cycles) [2]. Despite these advances, present Lithium-ion batteries could not fully overcome the EV range anxiety and battery with even higher energy density (higher range) are continuously demanded. A prospective solution is represented by the Lithium Sulfur (Li-S) battery technology [3].

Li-S batteries are characterized by very high theoretical specific capacity and gravimetric energy density of 1675 mAh/g and 2600 Wh/kg, respectively [3]. Furthermore, a practical gravimetric energy density of 400 Wh/kg has already been reached [4], which is almost two times more that of present Li-ion batteries. However, besides the aforementioned advantages, the Li-S chemistry suffers from fast capacity fade, poor efficiency, and high self-discharge [3], [5].

Thus, dynamic models, which are able to predict and assess the suitability and performance behavior of the Li-S batteries in various applications, such as EVs or light EVs, become necessary. Nevertheless, most of the models available in the literature are focused on understanding the polysulfide shuttle process, which governs and limits the performance of this battery technology [6]. To some extent, the availability of reliable dynamic models for Li-S batteries is limited [6], [7]. Furthermore, in all of these works, the electrical circuit model (ECM), which estimates the dynamics of the battery, is parametrized based on the DC pulse technique (i.e., a current pulse of a certain amplitude and duration is applied to the battery and the battery voltage response is recorded) [6], [7], [8].

An alternative approach for parameterizing the ECM of batteries is the use of the electrochemical impedance spectroscopy (EIS) technique [9], [10]. Most commonly, the EIS technique consists in applying to the battery a sinusoidal current of a certain amplitude and frequency and measuring its voltage amplitude and phase shift response; the procedure is repeated for a range of frequencies and thus the impedance spectrum of the tested battery is obtained and illustrated in the Nyquist plane. This technique presents a number of advantages over the DC pulse technique and it was successfully applied to parameterize the ECM of different Lithium-ion battery chemistries such as LFP [11], [12], LMO [13], LTO [11], [14], NMC [15], and NCA [16]. Furthermore, the EIS technique was applied also to Li-S batteries for battery characterization [17], [18] for electrochemical studies [19], [20], and for ageing analysis [5]. Nevertheless, to the best of our knowledge the suitability of the EIS technique for ECM modeling, of Li-S batteries, was not previously investigated .

Thus, in this paper, the EIS technique was used to parameterize, for a wide range of temperature and state-of-charge (SOC) levels, the ECM of a 3.4 Ah Li-S pouch cell. Once parameterized the parametrized model was verified for different mission profiles consideirng various temperatures and

load currents. More specifically, in this paper, we have developed a model to estimate the voltage of the Li-S cell during the discharge state. In comparison to the Lithium-ion chemistry, the voltage profile of Li-S batteries differs significantly between charging and discharging cases, as it is illustrated in Fig. 1. Consequently, only the later case was considered in the present work.

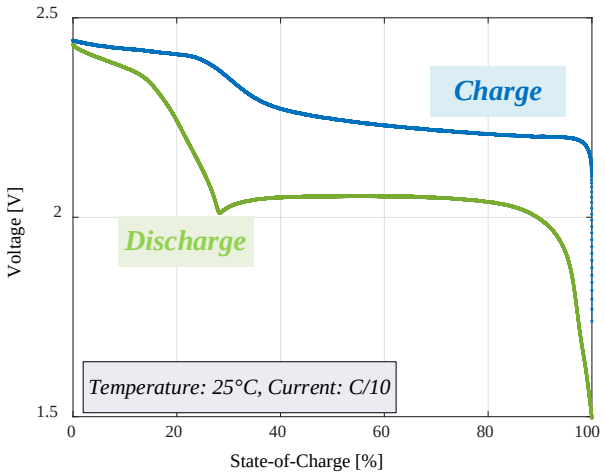

Fig. 1. Voltage profile of the Li-S battery cell during charging and discharging.

II. METHODOLOGY

A. Lithium-Sulfur Battery Under Test

This work was performed on a pre-commercial available 3.4 Ah long life type Li-S battery cell manufactured by OXIS Energy, which is presented in Fig. 2; the electrical parameters of this Li-S battery cell are presented in Table I. It has to be mentioned that all the tests were carried out under controlled temperature conditions, the cell have being placed inside a climatic chamber; furthermore, the temperature values mentioned in this work, are the ones measured on the surface of the battery and not the set-points of the climatic chamber.

B. EIS-based Characterization

The EIS measurements, were performed in galvanostatic mode (i.e., a small AC current is applied and the voltage response is measured), using a Digatron EIS analyzer, for the frequency range 6.5 kHz – 10 mHz for a total of 48 frequency points. All the measurements were carried out without superimposed DC current. These measurements were further used to determine the values of the elements of the equivalent electrical circuit (EEC), which is responsible for predicting the dynamic behavior of the Li-S battery cell.

A typically measured impedance spectrum corresponding to the tested Li-S battery cell is presented in Fig. 3; the Nyquist curve is composed of a depressed semi-circle in the high frequency region (6.5 kHz – 205 Hz), a second depressed semi-circle in the middle frequency range (205 – 0.36 Hz), and a quasi-straight line in the low frequency region (0.36 Hz – 10 mHz).

TABLE I. ELECTRICAL PARAMETERS OF THE TESTED LI-S BATTERY CELL

Parameter	Value
Type	Pouch
Nominal Capacity	3.4 Ah
Nominal Voltage	2.05 V
Maximum Voltage	2.45 V
Minimum Voltage	1.5 V
Nominal Charging Currentt	0.34 A (0.1 C-rate)
Nominal Discharging Current	0.68 A (0.2 C-rate)

EIS measurements were performed for four temperatures levels (i.e., 15°C, 25°C, 35°C, and 45°C) and for the whole SOC interval, with 5% SOC resolution. The dependence of the battery cell's impedance spectra on the temperature and SOC is illustrated in Fig. 4 and Fig. 5, respectively.

In order to parameterize the EEC for the tested Li-S battery, the measured impedance spectra had to be curve fitted. The EEC presented in Fig. 6 was proposed for curve fitting, as it was able to reproduce most accurately the battery's measured impedance spectra [17]. An example of the curve fitting results, illustrating the accurate match between the measured and estimated impedance spectrum, is presented in Fig. 6. The accuracy of the curve fitting process was assessed using the normalized root-mean square error (NRMSE). Depending on the EIS measurement condition (i.e., SOC and temperature), the NRMSE varied between 0.41 % and 2.33 %, with an average value for the 84 curve fitting cases of 0.96 %.

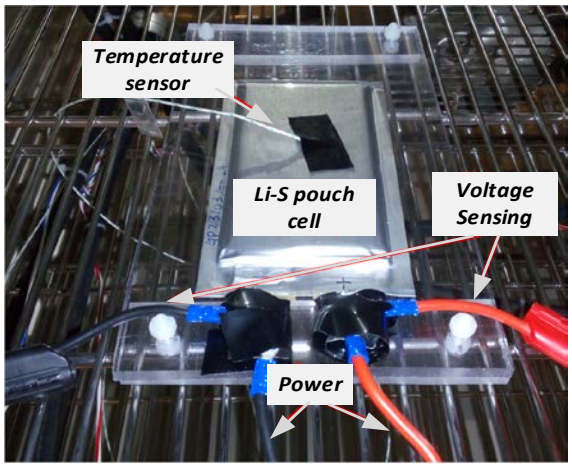

Fig. 2. Li-S pouch cell during the performance characterization tests.

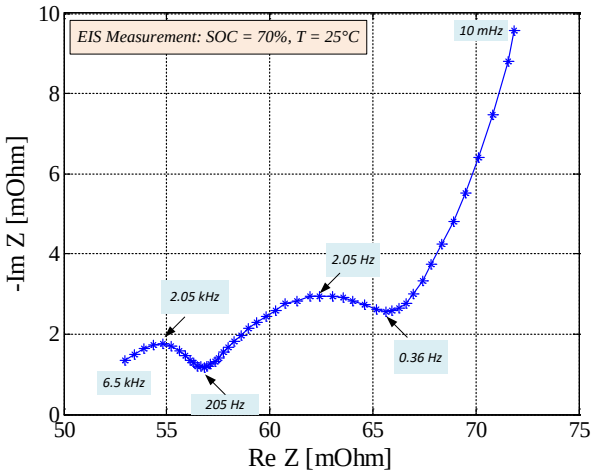

Fig. 3. Impedance spectrum of the tested Li-S battery cell.

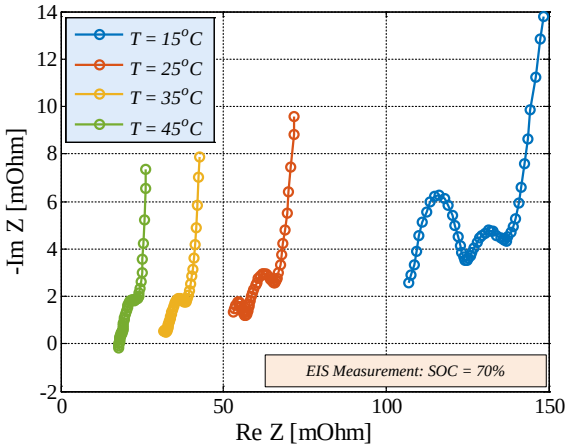

Fig. 4. Li-S battery cell impedance spectra measured at 70% SOC and various temperatures.

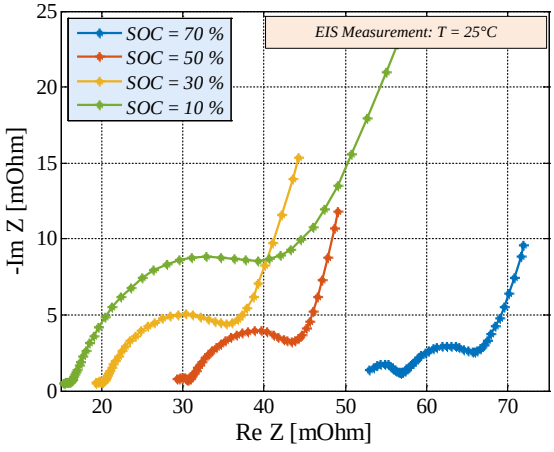

Fig. 5. Li-S battery cell impedance spectra measured at 25°C and various SOC levels.

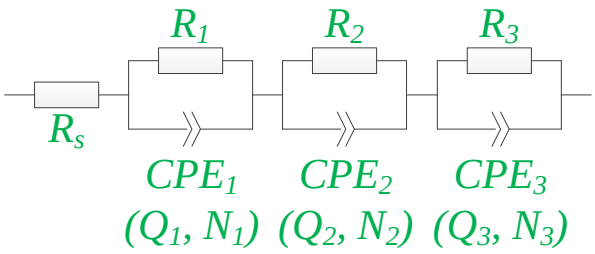

Fig. 6. Topology of the EEC used to fit the measured impedance spectra of the Li-S battery cell.

The variation of the EEC's parameters with the SOC and temperature was obtained by fitting all the measured impedance spectra, which were performed at various SOCs and temperatures. For exemplification, Fig. 8 presents the variation of the resistance R_s with SOC and temperature, which are in good agreement with the results presented in [21] by Wild et al. As it can be observed, the series resistance R_s increases exponentially with decreasing temperature – behavior, which is also encountered in the case of Lithium-ion batteries. Furthermore, independent on the measurement temperature, the resistance R_s increases with SOC until it reaches an inflection point at 70%-85% (depending on the temperature level), after which decreases steeply; this behavior is related to the viscosity of the polysulfide solution, which is the highest at this point as the result of the polysulfide species chain length and concentration [22].

C. Capacity and OCV Measurements

Besides the EIS characterization, measurements of the capacity and open-circuit voltage (OCV) were required in order to fully parameterize the ECM of the tested battery cell. The battery capacity was measured during discharging for different load currents (C-rates) by applying a constant current procedure; Fig. 9 presents the results obtained during the capacity measurements performed at 25°C for different C-rates. The same procedure was repeated at different temperatures. The OCV of the Li-S battery cell was measured by applying the GITT technique – i.e., the battery was discharged, from a fully charged state, using pulses of 3% SOC and applying two hours relaxation between the pulses. The obtained OCV vs SOC characteristic at 25°C and 0.5C pulse discharge is presented in Fig. 10.

Furthermore, it has to be mentioned that before all the previously presented measurements a pre-conditioning cycle was applied in order to reset the memory of the tested Li-S battery cell [23]. The pre-conditioning cycle was performed by fully charging the cell with a 0.1C current and fully discharging it with a 0.2C current.

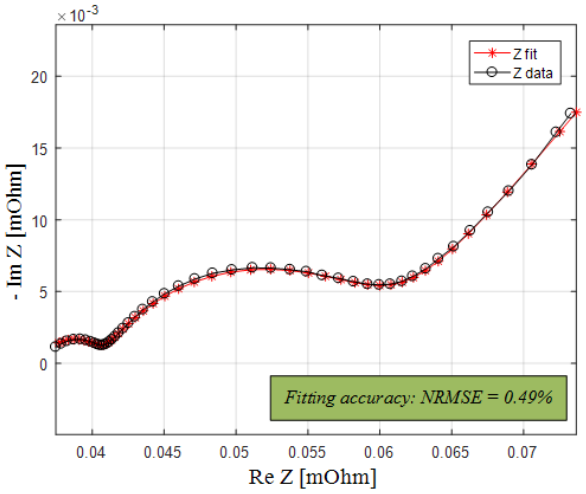

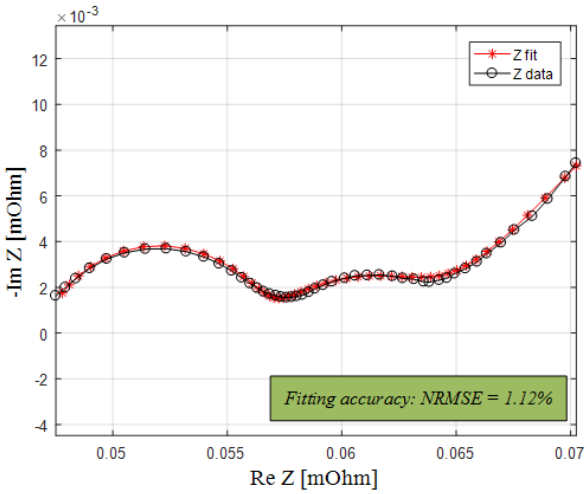

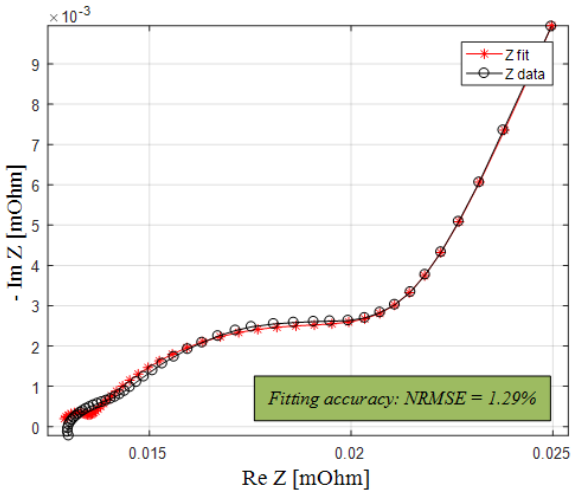

Fig. 7. Exemplification of the impedance spectrum curve fitting based on the EEC presented in Fig. 6 (T = 15°C and SOC =30% (top), T=25°C and SOC = 80% (middle), and T = 45°C and SOC =50% (bottom).

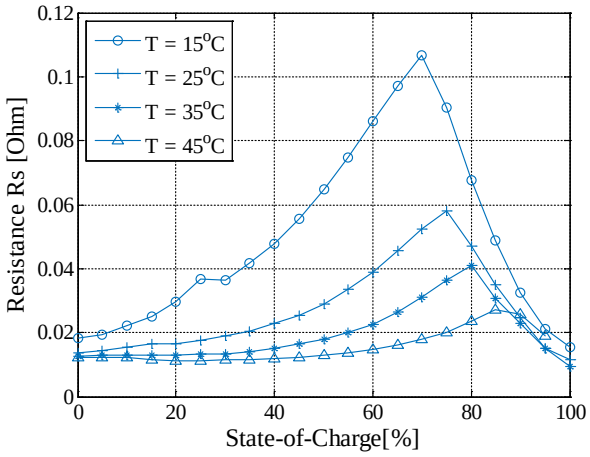

Fig. 8. Dependence of the resistance R_s on the SOC at different temperature values.

III. MODELING

The structure of the ECM, which was used to predict the discharging behavior of the studied Li-S battery cell is presented in Fig. 11. The left side of the model, presented in Fig. 11, composed from a capacitor and a current-controlled source was used to model capacity and the SOC of the Li-S cell. The voltage source in Fig. 11 is used to connect the SOC with the cell's OCV, while the EEC (whose elements are dependent on SOC and temperature) is used to estimate the dynamic behavior of the Li-S cell. Since only the battery discharging cases was considered in this work, the battery voltage was calculated according to (1).

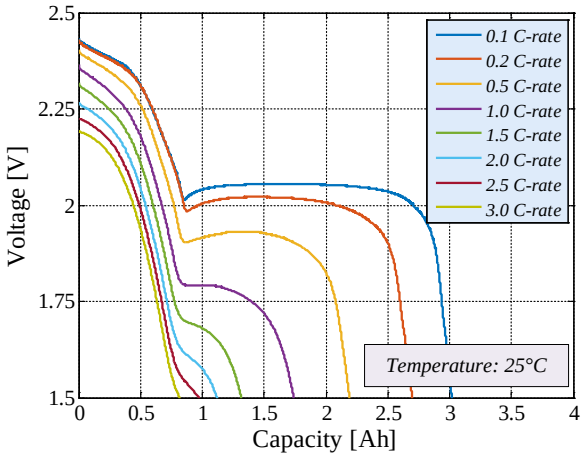

Fig. 9. Measured Li-S battery cell voltage profiles for different discharging C-rates.

Fig. 10.

$$V_{bat} = V_{OC} - Z_{EEC} \cdot I_{bat} = V_{OC} - V_{EEC} \quad (1)$$

Where, V_{bat} represents the voltage of the battery cell, V_{oc} represents the open-circuit voltage, Z_{EEC} represents the impedance of the EEC, I_{bat} represents the current flowing through the battery, and V_{EEC} represents the voltage drop across the battery's EEC.

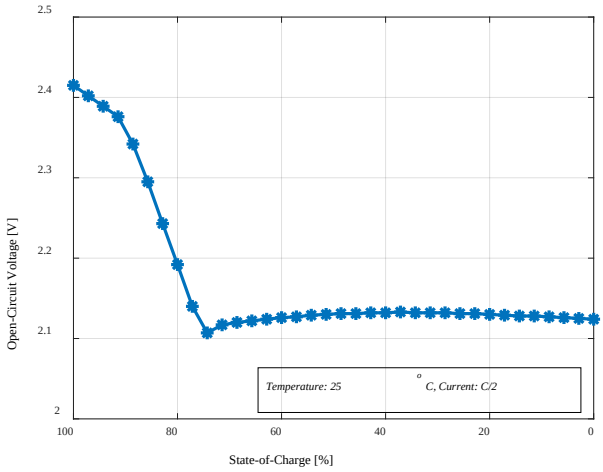

Fig. 11. Measured OCV vs SOC characteristic for the Li-S battery cell.

The ECM illustrated in Fig. 11 was implemented in MATLAB/Simulink. The parameters of the ECM (i.e., capacity, OCV, and elements of the EEC) have been implemented as 2D look-up tables in order to consider their variation with SOC and temperature.

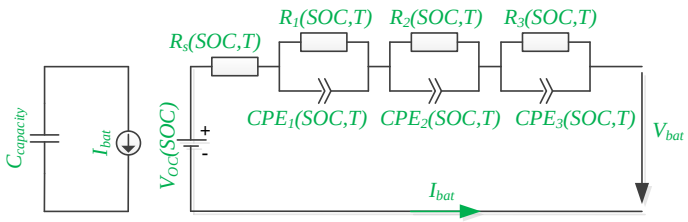

Fig. 12. ECM for estimating the Li-S battery cell voltage.

IV. Results

The performance of the developed and parameterized ECM for the 3.4 Ah Li-S battery cell was evaluated by means of simulation. Simulations using different load conditions were carried out and the results were compared with laboratory measurements performed under similar conditions (i.e., temperature and load current). Furthermore, the accuracy of the developed ECM was quantified by computing the mean percentage error (MPE) and the coefficient of determination R^2 according to (2) and (3), respectively.

$$MPE = \frac{100\%}{n}\sum_{i=1}^{n}\frac{|V_{model}\,(i) - V_{meas}\,(i)|}{V_{meas}\,(i)} \tag{2}$$

$$R^2 = 1 - \frac{\sum_{i=1}^{n}(V_{model}\,(i) - V_{meas}\,(i))^2}{\sum_{i=1}^{n}(V_{model}\,(i) - \overline{V_{meas}})^2} \tag{3}$$

where, V_{model} represents the battery voltage estimated by the model, V_{meas} represents the measured battery voltage, and n represents the number of voltage observation points.

A. Static Discharge

Firstly, the performance and accuracy of the proposed model were evaluated using static discharge conditions, i.e., the Li-S battery cell is discharged (until the minimum voltage is reached) from a fully charged state at different conditions (load currents and temperatures). The measured and estimated voltages of the Li-S battery cell for discharging at 25°C with three different C-rates (i.e., C/10, C/5, and C/2) are illustrated in Fig. 12. Furthermore, the measured and estimated voltage of the considered cell for discharging with C/2 at three temperatures (i.e., 15°C, 25°C, and 35°C) are presented in Fig. 13. As one can observe, the proposed model is able to predict the battery voltage with good accuracy during static discharge, independent on the considered C-rate and temperature; for the verification conditions presented in Fig. 12 and Fig. 13 a maximum MPE of 3.5% and minimum R^2 value of 0.982 were obtained. Moreover, it has to be mentioned that the major source of error is caused by the incapability of the model to predict the voltage around the inflection point between the high and low voltage plateau as well as for low SOCs (close to a fully discharged battery state).

B. Pulse Discharge

The second verification of the developed ECM was performed using a standard pulse discharge profile. From a fully charged state, the Li-S battery was discharged with pulses of 0.5 C-rate (1.7 Ah) until the minimum voltage was reached; between two discharging pulses, a relaxation period of 30 minutes was applied. The results of this verification test are presented in Fig. 14; similar to the previous case, the model is able to accurately predict the voltage of the considered 3.4 Ah Li-S battery cell (MPE = 3.8% and R^2 = 0.957). By comparing the two profiles, one can observe that the model has an overall tendency (during both pulse and relaxation period) to underestimate the voltage of the battery.

V. Conclusions

In this paper, we have proposed and parameterized an ECM for predicting the voltage behavior of a 3.4 Li-S pouch cell. While most of the literature available dynamic models for Li-S battery cells are parameterized using the DC pulse technique, in this work we have used the EIS method to parameterize the EEC (composed from a series resistance and three ZARC elements that are highly dependent on the SOC and temperature), which is responsible for the battery dynamic behavior. The ECM was parameterized for different temperatures and load current values by performing extensive laboratory characterization tests. By caring out two different verification tests (i.e., static and pulse discharge), it was shown that the proposed model is able to estimate with good accuracy the voltage of the tested battery cell. Consequently, EIS was validated as a reliable method for parameterizing the EEC of Li-S cells. In order to further improve the accuracy of the

proposed model, different aspects could be considered. For example, around the voltage inflection point between the high-voltage plateau and low voltage, a more precise parameterization could be done by considering a higher SOC resolution (e.g., 2% SOC) for both OCV and EIS measurements. Furthermore, as it could be observed, the behavior of the Li-S battery cell is highly-dependent on the temperature; thus, combining the developed electrical ECM with a battery thermal model will lead to an even better estimation of the voltage of the Li-S battery.

ACKNOWLEDGMENT

This work has been part of the ACEMU-project. The authors gratefully acknowledge the Danish Council for Strategic Research (1313-00004B) and EUDP (1440-0007) for providing financial support and would like to thank OXIS Energy for supplying the Lithium-Sulfur battery cells.

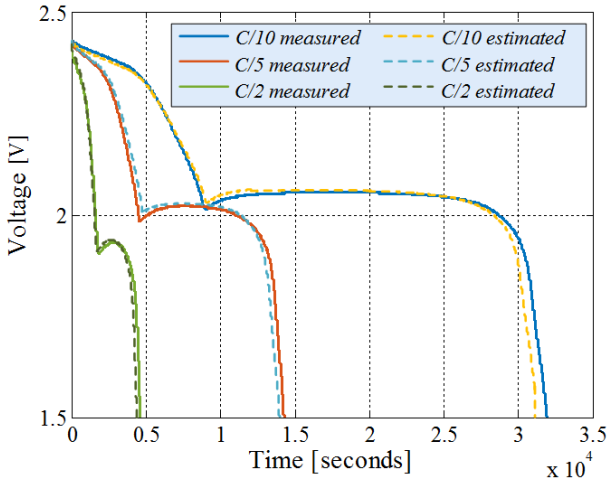

Fig. 13. Measured and estimated battery voltage for different C-rates and T=25°C.

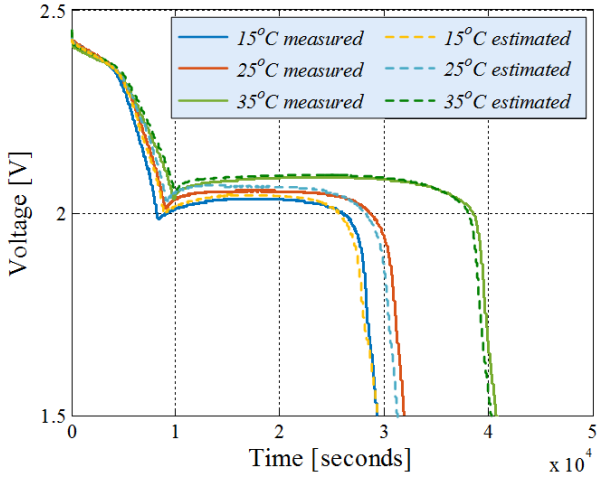

Fig. 14. Measured and estimated battery voltage for different temperates and C/10 C-rate.

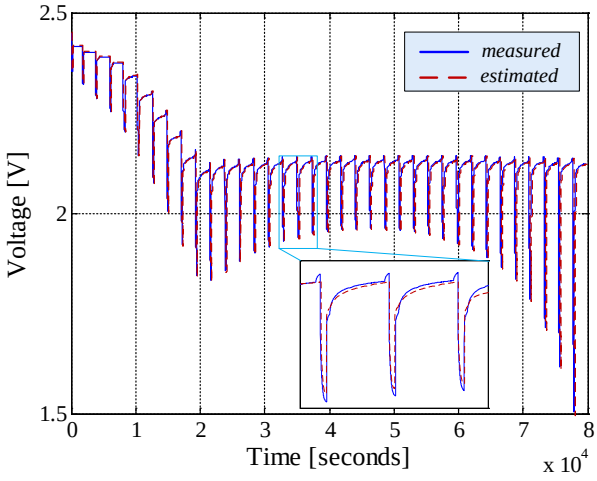

Fig. 15. Measured and estimated Li-S battery voltage for a pulse discharge profile (T = 25°C).

REFERENCES

[1] J. B. Goodenough and K.-S. Park, “The Li-Ion Rechargeable Battery: A Perspective,” Journal of American Chemical Society, no. 135, no. 4, pp. 1167-1176, 2013.

[2] A.-I. Stan et al., “Lithium Ion Battery Chemistries from Renewable Energy Storage to Automotive and Back-up Power Applications – An Overview,” 2014 International Conference on Optimization of Electrical and Electronic Equipment (OPTIM), pp. 713-720, 2014.

[3] P. G. Bruce, L. J. Hardwick, and K. M. Abraham, “Lithium-air and lithium-sulfur batteries,” MRS Bulletin, vol. 36, pp. 506-512, 2011.

[4] OXIS Energy Ltd., (accessed 15.01.17). URL: http://www.oxisenergy.com

[5] Z. Deng et al., “Electrochemical Impedance Spectroscopy Study of a Lithium/Sulfur Battery: Modeling and Analysis of Capacity Fading,” Journal of the Electrochemistry Society, vol. 160, no. 4, 2013.

[6] K. Propp et al., “Multi-temperature state-dependent equivalent circuit discharge model for lithium-sulfur batteries,” Journal of Power Sources, vol. 328, pp. 289-299, 2016.

[7] V. Knap et al., “Electrical Circuit Models for Performance Modeling of Lithium-Sulfur Batteries,” 2015 IEEE Energy Conversion Congress and Exposition (ECCE), Montreal, QC, 2015, pp. 1375-1381.

[8] A. Fotouhi et al., “Lithium-Sulfur Cell Equivalent Circuit Network Model Parametrization and Sensitivity Analysis,” IEEE Transactions on Vehicular Technology, vol.PP, no.99, pp.1-1, 2017.

[9] E. Barsoukov and J.R. Macdonald, “Impedance Spectroscopy. Theory, Experiment and Applications,” Wiley 2005.

[10] D.-I. Stroe, V. Knap, M. Swierczynski, and E. Schaltz, ”Electric circuit modeling of lithium-sulfur batteries during discharging state,” 2017 IEEE Energy Conversion Congress and Exposition (ECCE), Cincinnati, OH, 2017, pp. 1024-1029.

[11] M. Świerczyński, et al, "Selection and Performance-Degradation Modeling of $LiMO_2/Li_4Ti_5O_{12}$ and $LiFePO_4$/C Battery Cells as Suitable Energy Storage Systems for Grid Integration With Wind Power Plants: An Example for the Primary Frequency Regulation Service," IEEE Transactions on Sustainable Energy, vol. 5, no. 1, pp. 90-101, Jan. 2014.

[12] T.K. Dong, A. Kirchev, F. Mattera, J. Kowal, and Y. Bultel, “Dynamic Modeling of Li-ion Batteries Using an Equivalent

Electrical Circuit," Journal of the Electrochemical Society, vol. 158, no. 3, A326-A336, 2011.

[13] S. Buller et al., "Impedance-Based Simulation Models of Supercapacitors and Li-Ion batteries for Power Electronic Applications," IEEE Transactions on Industry Applications, vol. 41, no. 3, 2005.

[14] A.-I. Stroe, M. Swierczynski, D.-I. Stroe, R. Teodorescu, "Performance Model for High-Power Lithium Titanate Oxide batteries based on Extended Characterization Tests," 2015 IEEE Energy Conversion Congress and Exposition (ECCE), Montreal, Canada, 2015, pp. 6191-6198.

[15] G. Perez, I. Gandiaga, M. Garmendia, J.F. Reynaud, U. Viscarret, "Modelling of Li-ion batteries dynamics using impedance spectrosopy and pulse fitting: EVs application," 2013 World Electric Vehicle Symposium and Exhibition (EVS27), Barcelona, 2013, pp. 1-9

[16] D. Andre et al., "Characterization of high-power lithium-ion batteries by electrochemical impedance spectroscopy. II. Modelling," Journal of Power Sources, vol. 196, no. 12, pp. 5349-5356.

[17] D.-I. Stroe et al., "An Electrochemical Impedance Spectroscopy Study on a Lithium Sulfur Pouch Cell," ECS Transactions, vol. 72, no. 12, pp. 13 – 22, 2016.

[18] N. A. Canas et al., "Investigation of lithium-sulfur batteries using electrochemical impedance spectrosocpy," Electrochemica Acta, vol. 97, pp. 42-51, 2013.

[19] J. Conder et al., "Electrochemical impedance spectroscopy of a Li-S battery: Part 1. Influence of the electrode and electrolyte compositions on the impednace of symmetric cells," Electrochemica Acta, vol. 244, pp. 61-68, 2017.

[20] S. Walus, A. Robba, R. Bouchet, C. Barchasz, F. Alloin, "Infleunce of the binder and preparation process on the positive lectrode electrochemical reponse and Li/S system performance," Electrochemica Acta, vol. 210, pp. 492-501, 2016.

[21] M. Wild et al., "Lithium sulfur batteries, a mechanistic review," Energy & Environmental Science, vol. 8, no. 12, pp. 3477-3494, 2015.

[22] Z. Zhang, "Liquid electrolyte lithium/sulfur battery: Fundamental chemistry, problems, and solutions," Journal of Power Sources, vol. 231, pp. 153-162, 2013.

[23] V. Knap et al., "Methodology for Assessing the Lithium-Sulfur Battery Degradation for Practical Applications," ECS Transactions, vol. 77, no. 11, pp. 479-490, 2017.